Resolving the Thickness of Submarine Lava Flows in the North Arch Volcanic Field Using Magnetometry

Reese Miller

Rjmill7@uw.edu

Senior Thesis

University of Washington

School of Oceanography

Seattle, WA 98105

Abstract

The North Arch Volcanic Field is a part of the greater Hawai'ian volcanic arch north of O'ahu. Only discovered in the 1960s; relatively little is known about it and the arch volcanism that formed it. One general property of basaltic lava flows is their relatively high remnant magnetization which distinguishes them from the surrounding, weakly-magnetized sediments. It was predicted that these flows would produce strong enough anomalies to be detected from surface level and that the resolved flows would have thicknesses in the 10s of meters. The ship followed a series of 5 track lines of 15-40 km heading in the east-west direction before traveling north-west along an inferred eruptive fissure. 29 lava flows were identified through sub-bottom profiler data. After collection, the data was processed in GRAV_MAG_PRISM, a modeling program which allows the user to break a magnetic body into prisms. Models were first created to assess what size lava flows would correspond to the average anomaly found in the data. Afterwards, one surveyed flow was modeled, and the prisms were manipulated to see if the modeled data could accurately match the collected data. Yielding thicknesses along the flow ranging from 5 to 50 meters, confirming predictions about their relative thickness. The results of this study demonstrate that magnetometry can be an effective tool for studying the North Arch Volcanic Field. In the broader scientific context, this also shows that magnetometry could be used on other submarine volcanic fields as well.

Plain Language Summary

The North Arch Volcanic Field lies above the Hawai'ian Island of O'ahu. This wide area of the seafloor is notable for its high levels of volcanic activity, and large quantities of long lava flows. Volcanism is important to study as it played a major role in shaping the Earth and still affects our lives today, often in the form of a natural hazard. Understanding volcanism, even in a non-hazardous context, can help us understand and plan for hazardous volcanism. The North Arch was only discovered in the 1960s and not much research has been conducted here. The goal of this study was to contribute data about North Arch lava flows by modeling their thickness. This was done using a magnetometer, which measures magnetic anomalies (magnetic signals that vary from the Earth's magnetic field). Earth's magnetic field changes over time, however basalt, what most lava flows are made of, tends to retain the field strength and direction when it cools (known as remnant magnetization). As such, basalt is strongly magnetized while seafloor sediments are only weakly magnetized. Therefore, it is easy to distinguish between lava and sediments using magnetic anomaly data. Lava flow thickness was determined by running the collected data through a modeling program. The final model fit the collected data rather well. Results showed that the modeled flow was thin but that it gave off a strong enough anomaly to be detected from the sea surface. This work can be used to better understand how North Arch volcanism works.

Introduction

Volcanism and processes that lead to it play an integral role in shaping the Earth. Mantle circulation is a driving force behind plate tectonics, the process which shapes our planet, creating the continents and ocean basis. Tectonics also lead to the creation of mid ocean ridges and subduction zones where volcanism is most common (Meschede 2016). Volcanism, both terrestrial and submarine, is also of immense importance to life on Earth. Terrestrial volcanism is a defining presence of human existence, both in the local hazards it presents and the wide-spread impacts that volcanism can have on climate (Eldholm and Coffin 2016). Mid ocean ridge magmatism and volcanism are responsible for the creation of new ocean crust and the formation of the ocean basins, as well as in defining the morphology of the sea floor. Other forms of submarine volcanism, such as hotspot volcanism, are responsible for the creation of many island chains which have long been inhabited by humans. Additionally, hydrothermal vent systems, a form of submarine volcanic system are considered as a plausible location for where the origin of life occurred (Koschinsky 2016). Needless to say, Earth could not exist as it currently does without volcanic processes, making them a vital area of research if we wish to fully understand our planet, especially the seafloor where the majority of volcanism takes place (Helo 2016).

The Hawai'ian Islands, the area of focus for this project, were formed by upwelling from a mantle hotspot which has led to volcanism both terrestrial and submarine (White 2016). Two offshore regions, the South and North Arch Volcanic Fields, were formed through volcanism from the Hawaiian hotspot as well (Bianco et. al. 2005). The North Arch Volcanic Field lies north of O'ahu, covering a total area of approximately 24,000 km^2 (Clague et. al., 2002) (Figure 1). Despite encompassing a large swath of the seafloor, this area has been relatively understudied.

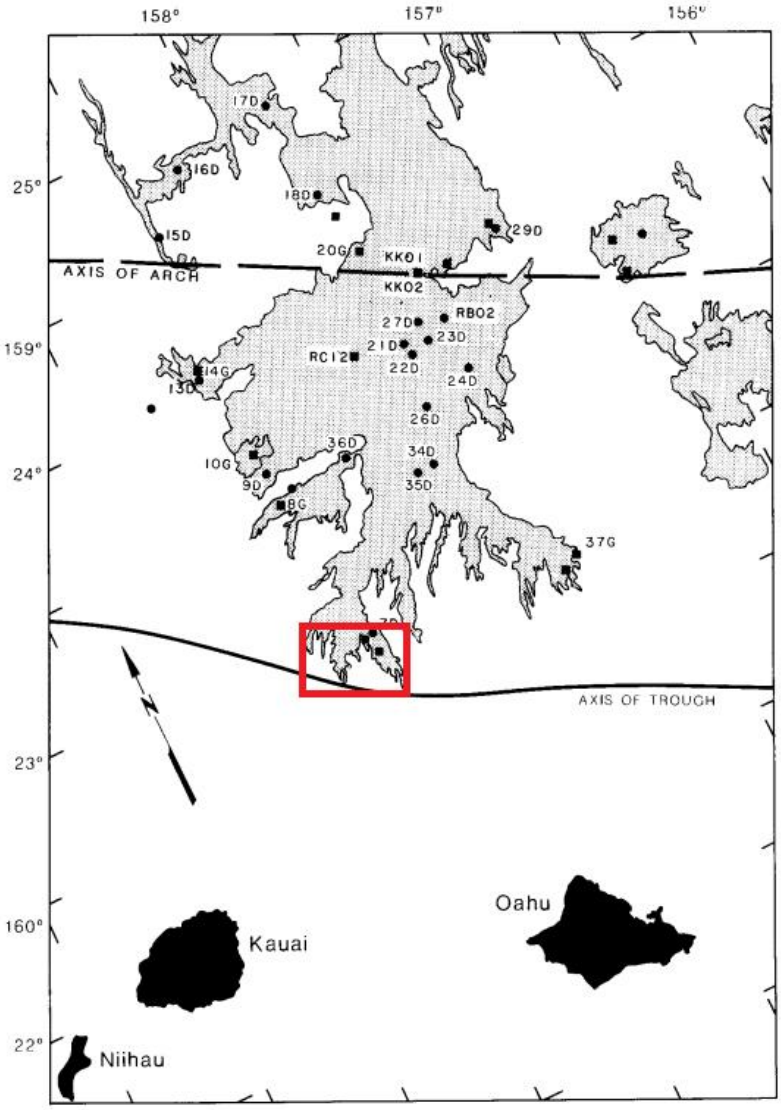

Figure 1. A map of the North Arch and its location relative to the Hawaiian Islands. The area in the red box is the approximate location of this survey (Clague et. al. 1990).

The North Arch was first discovered using seismic reflection imaging in 1968. This study revealed that there were large areas of little to no sedimentation north of O'ahu which was predicted to be a result of volcanic activity (Normark and Shor 1968). It wasn't until 1982 that these areas were confirmed to be lava flows, using a combination of seismic reflection and echo sounder data (Wallin 1982). Following the North Arch's discovery there were several surveys along the Hawaiian arch which utilized the GLORIA side scan system to produce backscatter images of the sea floor (Normark et al. 1989). As further research revealed the

complexity of the North Arch, many wondered how the region could have formed in the first place.

The North Arch Volcanic Field likely is product of the Hawaiian hotspot that built the Hawaiian Islands through a process known as arch volcanism, a type of secondary volcanism which occurs after a period of volcanic inactivity (Bianco et al. 2005). One theory for its formation is that North Arch was formed by a particular type of secondary volcanism known as small scale sublithospheric convection (SSC) which would allow for volcanism even far away from the main mantel plume (Ballmer et. al., 2011). Hotspots are formed when a plume of material from the mantle rises; as the pressure decreases the plume can melt through the overlying lithosphere eventually reaching the seafloor in a process known as decompression melting (White, 2016). As the name implies, SSC is a small-scale version of this (Ballmer et. al., 2011). In the small-scale process, the lithosphere develops a "washboard" pattern from small sections of mantle circulation unrelated to the hotspot. Over time, the hotspot plume can start to spread horizontally and interact with the washboard lithosphere where it is 'drawn' to the thin sections of lithosphere. This leads to further decompression melting and volcanism. Through SSC, mantle material is drawn away from the hotspot, offering a potential explanation for how such extensive secondary volcanism can be occurring away from the Hawaiian hotspot. Another theory is that the North Arch's volcanism is derived from material in the core of the plume which has become particularly hot and viscous as a result of dehydration induced by the plume's melt of the lithosphere. This has been called 'restite-root' hypothesis, where the root is the viscous core of the plume. It was found that the models of restite-root processes were able to account for sustained volcanism on the young side of a fracture zone. This finding is applicable to the North

Arch, which lies on the younger side of the Molokai fracture zone (Yamamoto and Morgan 2009).

Following the GLORIA surveys, there was a more intensive mapping effort conducted in 1999 using a SeaBeam 2100 mapping system (Clague et. al., 2002). This survey was solely focused on the North Arch and contributed much needed data about the region's bathymetry (Figure 2). The early surveys revealed the presence of several long lava flows around the Hawaiian Islands (Holcomb et. al. 1988). Results from the 1999 survey, showed that the North

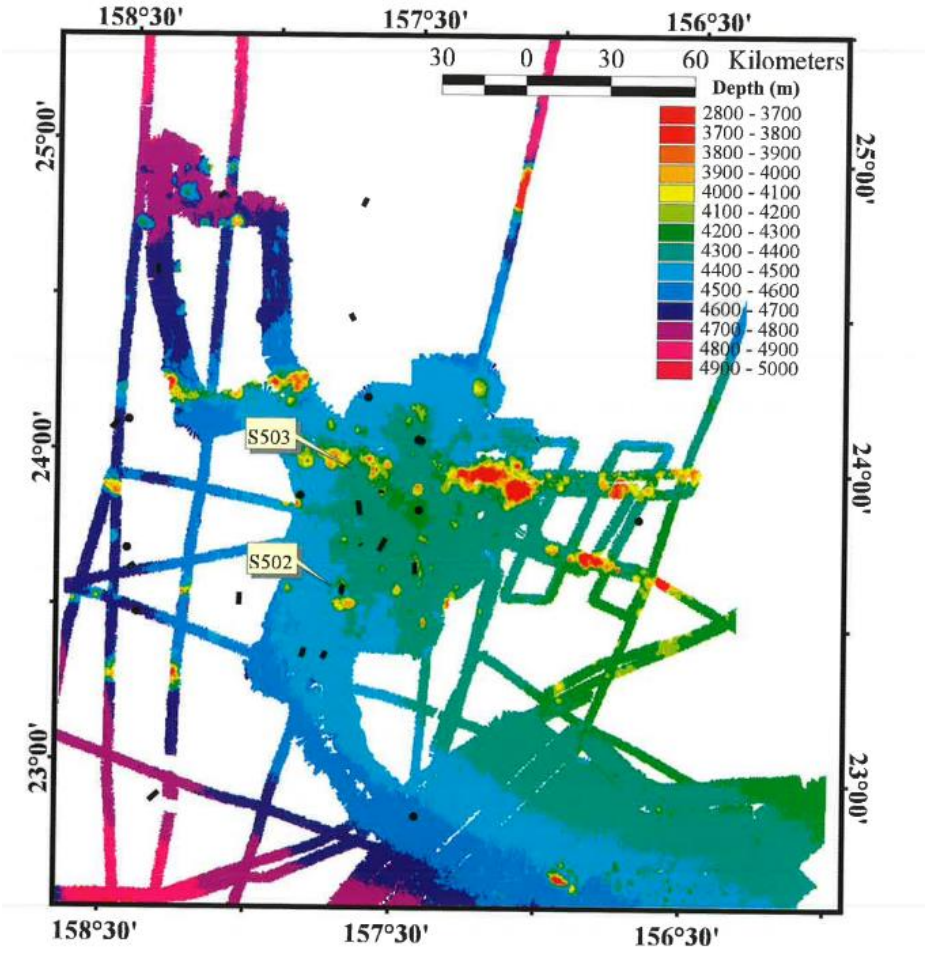

Figure 2. Map of North Arch bathymetry compiled after a 1999 survey of the area (Clague et. al. 2002). While there were significant contributions to data about the North Arch, much of it remains unmapped.

Arch hosts some of the world's longest submarine lava flows, with one flow in the northwestern region reaching 108 km (Clague et. al. 2002).

In the submarine environment long flows, defined as being longer than 100 km, can form more easily than in a terrestrial setting (Gregg and Fornari 1998). There are two primary reasons for this: high pressures on the seafloor and rapidly cooling of the lava's outer layer. High pressures prevent dissolved volatiles from expanding and creating vesicles. This would increase the lava's viscosity but decrease its flow velocity and therefore its length. Rapid cooling of the lava flow upon contact with cool seawater, solidifies the outer layer creating a glassy crust which serves as insulation for the lava inside. This glassy crust is what makes most submarine lava flows volume limited rather than cooling limited. It has been found that of the three types of lava flows (sheet, lobate, and pillow), sheet flows tend to travel the furthest. This is reasonable considering the impact of flow velocity on flow length.

Flow length is correlated with flow velocity (Figure 3) (Gregg and Fornari 1998). Sheet flows travel quickly over a brief period and tend to have high velocities, owing to high magma effusion rates (McClinton et. al. 2014). Another important control on length is viscosity, with low viscosity lavas, such as those within the crusts of rapidly cooled flows, able to travel further (Gregg and Fornari 1998). Viscosity is one of the major controls on flow morphology in general, with impacts on thickness as well. Sheet lows have relatively uniform thickness, however for volume limited flows it seems reasonable to predict that the edges of flows will be thinner as magma supply is depleted. Given these factors, North Arch flows, which are relatively long, will likely have thicknesses in the 10's of meters.

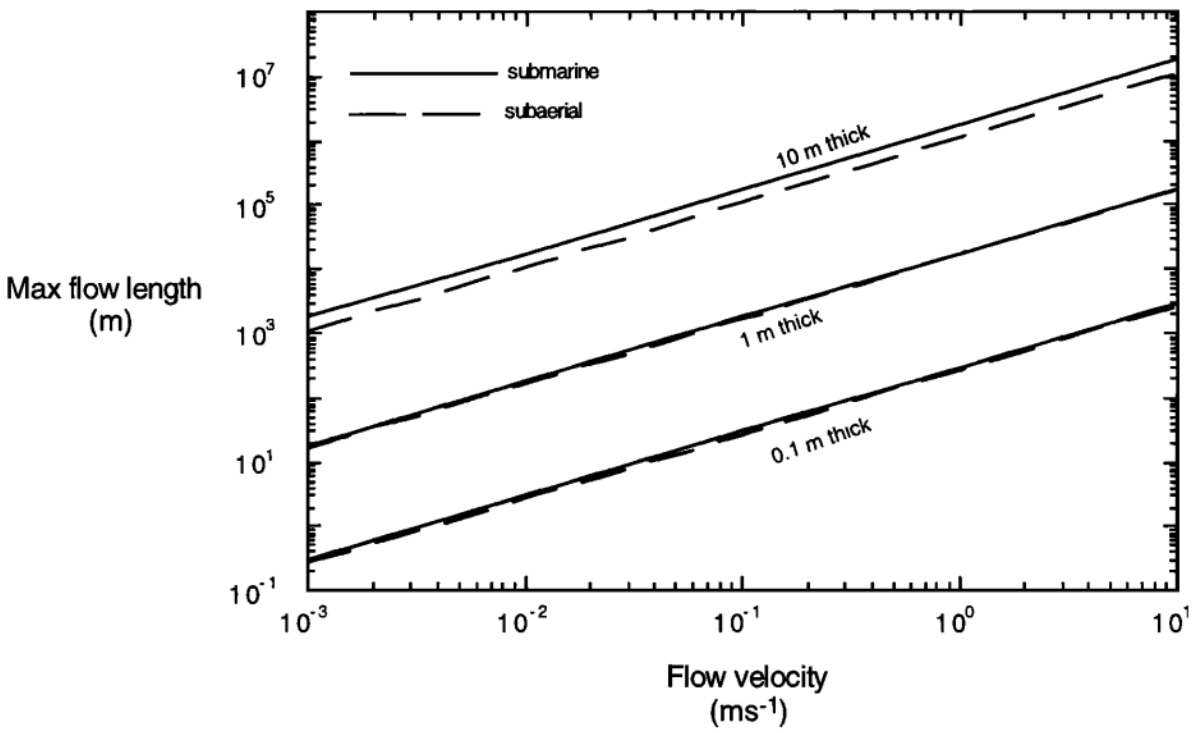

Figure 3. Velocity versus the max flow length of lava flows in both the submarine and subaerial environments. Given that the North Arch contains several long lava flows, flows are likely to be 10 or more meters in thickness (Gregg and Fornari 1998)

An effective method for determining the thickness of lava flows is using magnetometry (Tivey et. al., 1998). When lava flows are emplaced, they retain records of the Earth's magnetic field at the time, known as a magnetic anomaly. Basaltic lava flows contain magnetite, a mineral that retains magnetism from the Earth's magnetic field once cooled below its Curie temperature of 578 °C (Kearey et al. 1984). Sediments surrounding lava flows are very weakly magnetic, and in theory it is possible to identify lava flows by looking at the magnetic anomalies, which will be much higher over the lava flows. The magnetism of lava flows does decrease with age, making their anomaly signal weaker. However, the lava flows in the North Arch are geologically young, 0.75 – 2.7 Ma (Clague et. al. 1990) and are covered by a relatively thin layer of sediment, less than

200 m in most places, which represents relatively slow sediment accumulation (Wallin 1982). The data gathered by the magnetometer can then be turned into magnetically derived flow thickness maps using modeling (Tivey et. al. 1998) (Figure 4). The survey that initially performed this type of study surveyed lava flows using a bottom scanning autonomous underwater vehicle (AUV). This survey was conducted using a surface scanning magnetometer, which cannot detect the smaller scale anomies that a bottom scanner can. However, based on previous studies conducted in the area and on lava magnetization in general, I hypothesized that the North Arch flows would have large enough anomalies to be detectable, even from surface level. From these anomalies it would also likely be possible to characterize their thickness, as previous studies have done so in the past. Additionally, based on flow length to thickness relationships, the detected flows are likely to be 10s of meters thick.

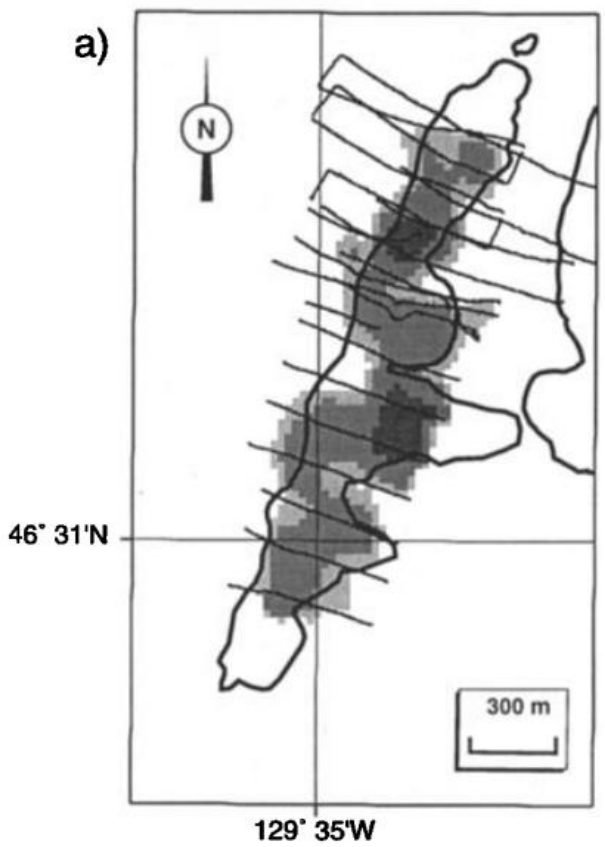

Figure 4. Example of magnetically derived lava flow thickness map from a study along the Juan de Fuca Ridge. Data was collected using a bottom scanning AUV, this study will be using a surface towed magnetometer (Tivey et. al. 1998).

Methods

Data collection was started on December 19th, 2021, in the southern portion of the North Arch (Figure 5). The ship followed 5 east-west track lines ranging from approximately 15 to 40km long before traveling north-west for 60 km along an inferred eruptive fissure then exiting the volcanic field. A 30 kHz Kongsberg EM-302 Echosounder Multibeam system, a 3.5 kHz

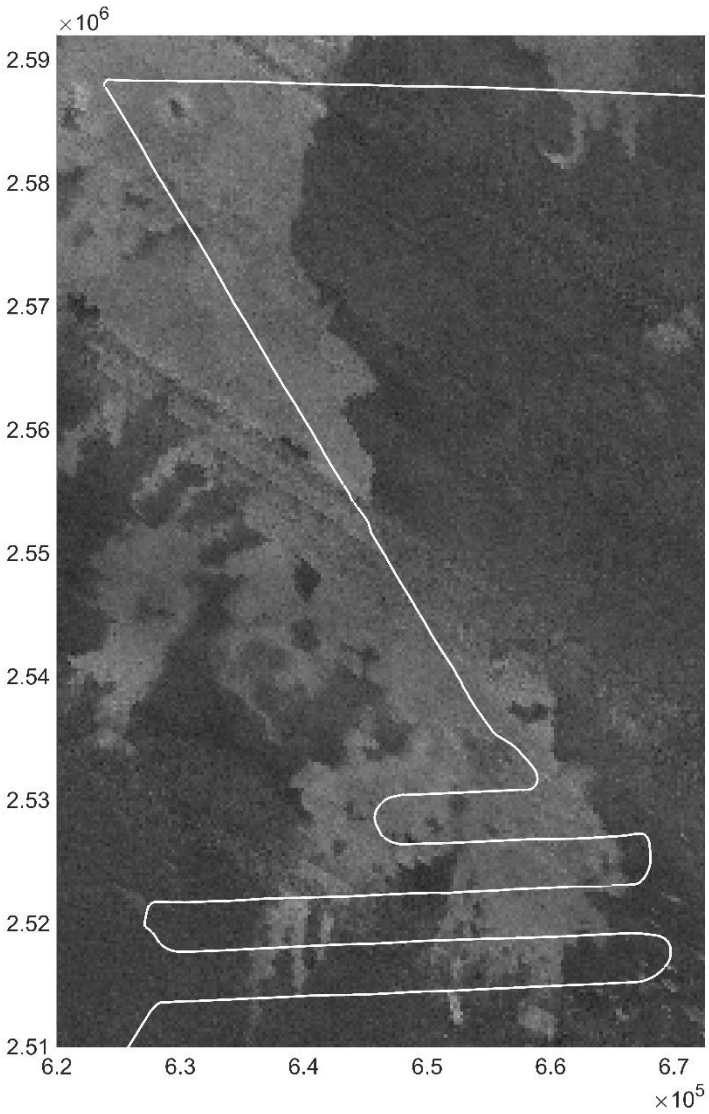

Figure 5. Survey plan which the ship followed mapped on top of existing GLORIA data (Clague et. al. 2002). The ship followed several track lines in a zig-zag pattern to collect data over lava flow boundaries. The ship then travelled straight north-west along an inferred fissure. The axes are in UTM, a measurement of distance which can be approximated as meters.

Knudsen sub-bottom profiler, and a Seaspy Marine Magnetometer System were used to collect multibeam, sediment, and magnetic data respectively. The magnetometer was towed behind the ship and collected data from surface level. A bathymetry map was created using the multibeam data (Figure 6). Afterwards, the sub-bottom profiler data was analyzed to locate lava flow boundaries, which were then placed on the bathymetry map (Pfluger, 2022).

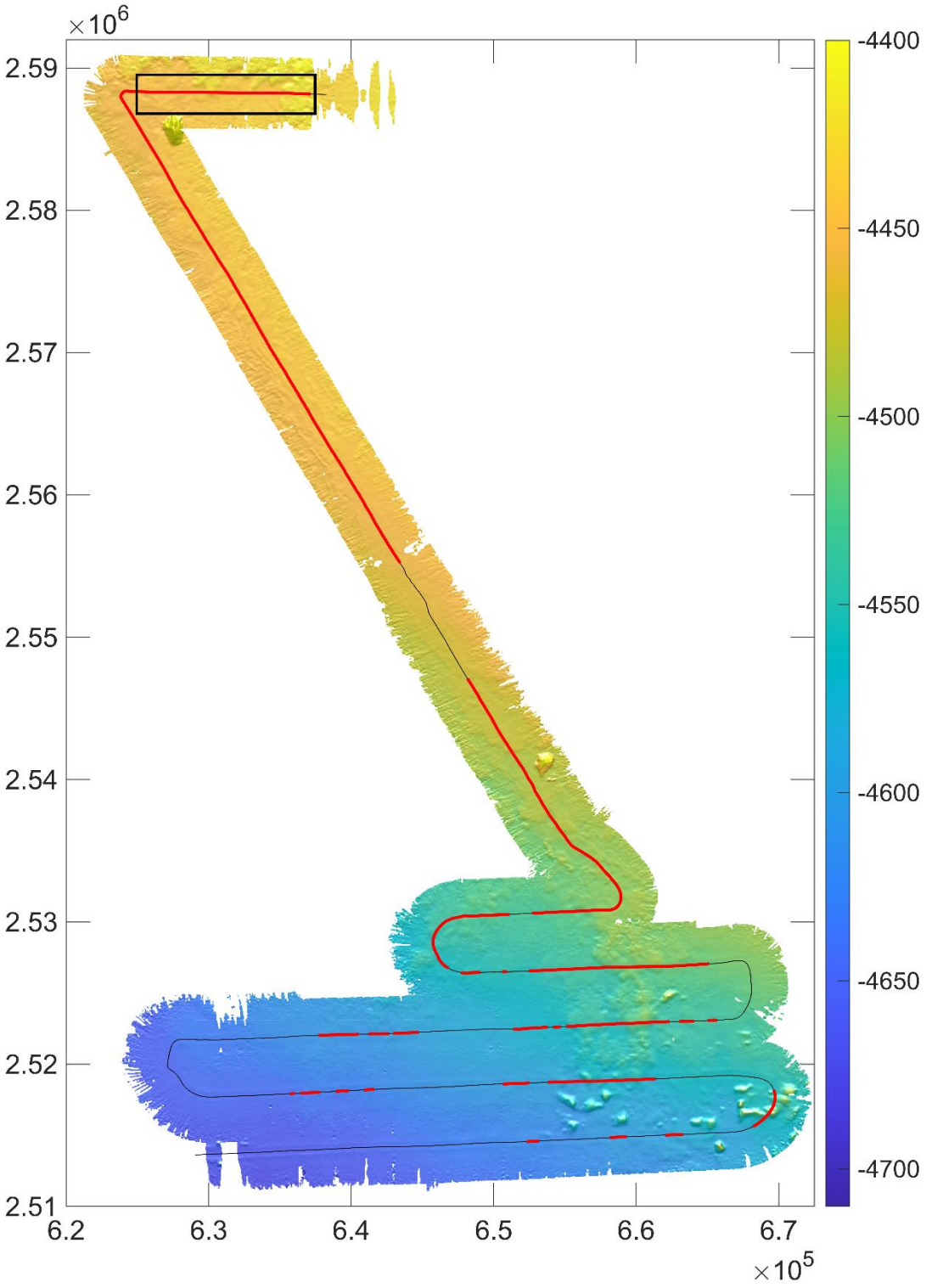

Figure 6. Bathymetry data from the survey, including track lines with red sections indicating lava flows. Due to difficulties with swell, data along the edges of the swath is of lower quality. The black box indicates roughly which section of the lava flow was modeled.

To begin processing the magnetics data, corrections had to be made to account for variations in the Earth's magnetic field. This was done using International Geomagnetic Reference Field (IGRF) data, local short term and diurnal magnetic variation readings from the Honolulu magnetic observatory, the nearest observatory to the survey area.

The first modeling phase involved the creation of several models for hypothetical East-West and North-South trending lava flows which will be referred to as generic models. These hypothetical flows were assigned a remnant magnetization of 40 A/m, based on previous magnetic measurements from Icelandic basalt, a decent approximation given that there is no existing data on North Arch remnant magnetization (Gunnlaugsson et. al. 2006). Water depth was also held constant. The range of widths were chosen, and then various thicknesses were tested with each width to assess the range of dimensions that a lava flow with anomalies similar to those measured in the North Arch could have.

Next, one section of the data collected over a lava flow was chosen for further analysis. This data was run through the GRAV_MAG_PRISM modeling program, which breaks a magnetic body into several rectangular prisms (Biangolo et. al. 2013). The thicknesses of these prisms were then manipulated to create a model of the lava flow. The anomalies produced by this model were then compared to the real anomaly data to assess how well the model fit. All parameters including flow area, azimuth, remnant magnetization (40 A/m) were held constant so that thickness was the only parameter of each prism that could be manipulated.

Results

Variations in the IGRF, diurnal and short-term magnetic fields (Figures 7B, 7C) were all relatively small. This is important to note as larger variations, such as those caused by a magnetic

storm, would have made the collected data very difficult to use. Another profile was made of the corrected data, this time combined with the sub-bottom profiler data, to show which sections of data were collected over lava flow boundaries (Figure 8). This initial processing of the magnetics data showed that the surveyed lava flows had average magnetic anomalies of ±25 nT.

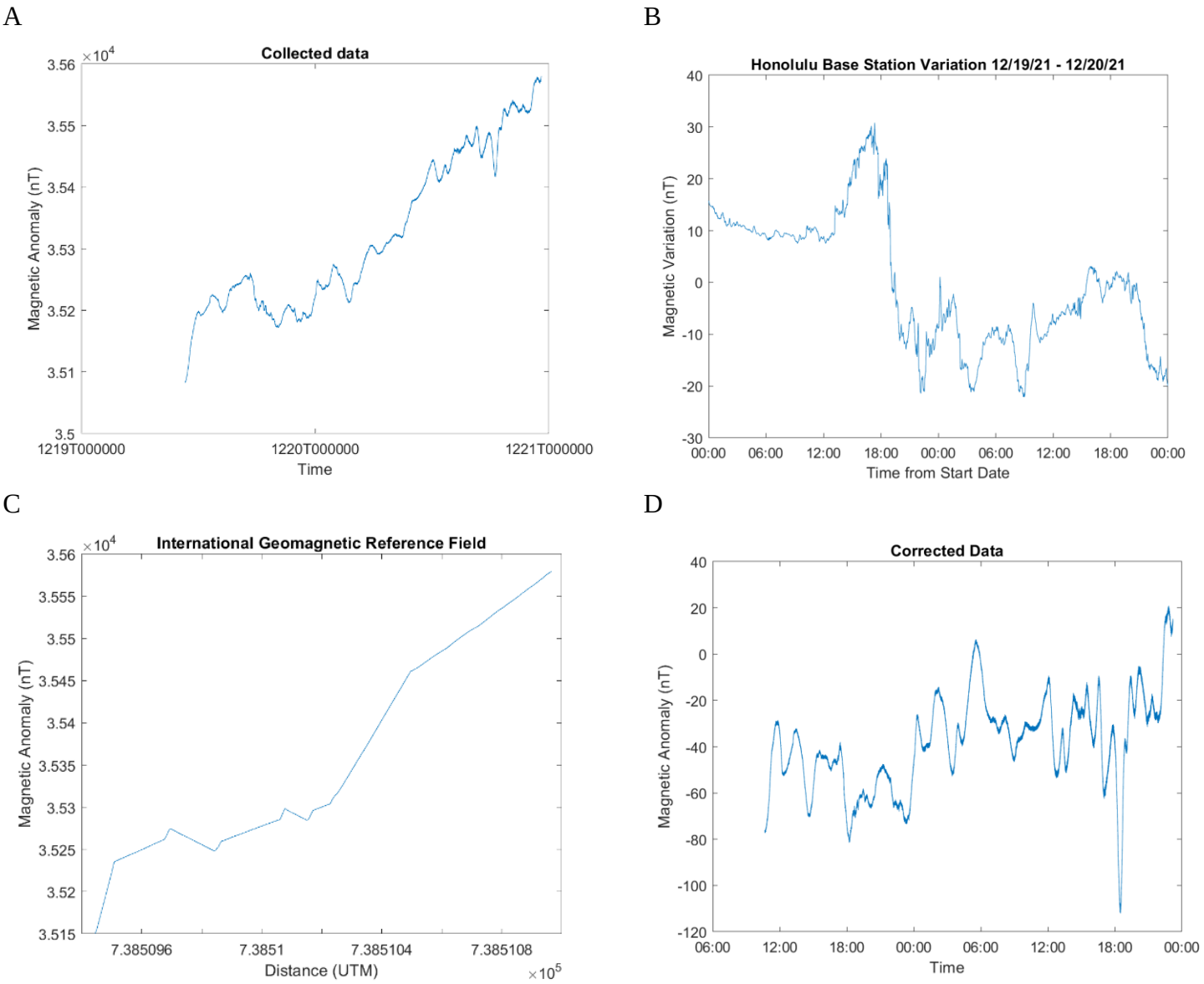

Figure 7. A) Raw data collected by the magnetometer. B) Variations in the local magnetic field during the survey period collected by the Honolulu magnetic observatory. C) IGRF data along the survey track showing magnetic variations by distance. D) The final data after the Honolulu and IGRF variations were taken out of the raw data.

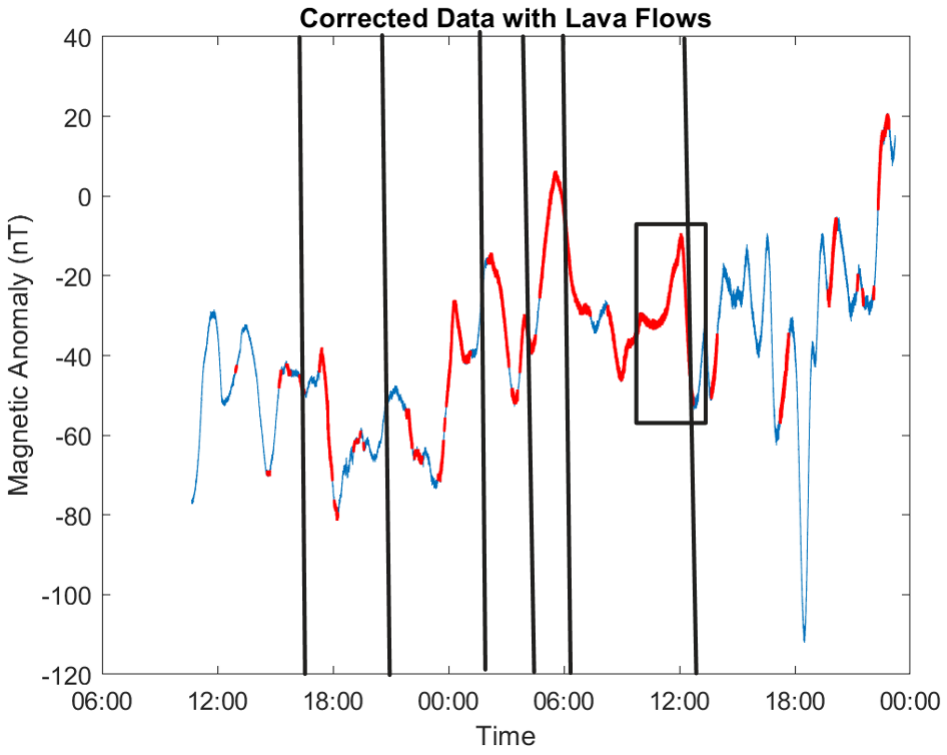

Figure 8. Corrected data overlain with the lava flows identified by the sub-bottom profiler, shown by the red lines. The black vertical lines indicate when the ship was in a turn and the black box highlights the lava flow that was mapped. While there are several distinct red lines show, most of these were not individual flows, but parts of larger flows.

The generic models with the most realistic parameters (i.e., with widths and thicknesses that produced the right anomaly signature without having highly unrealistic dimensions) served as a baseline for the actual lava flow model. Figure 9 shows an east-west profile through a hypothetical north-south (NS) lava flow. This flow is normally magnetized with a width of 5000 m and a thickness of 38 m, which produced a maximum positive anomaly of 24 nT. Figure 10 shows a north-south profile though an east-west (EW) lava flow, also normally magnetized. This flow is 2500 m and thickness of 45 m with a maximum positive anomaly of 25 nT. The models shown are only two of several hypothetical flows that fit the anomaly size shown in the collected data. Table 2 lists the full range of parameters tested that fell within the ±25 nT anomaly range.

Table 2. A table of the combinations of thicknesses and widths for both the NS and EW models that produced a roughly ±25 nT anomaly. Flows thinner than 1-2 km are unlikely as these flows would then have to be unreasonably thick to produce the correct anomaly.

North-South Models								
Width (m)	100	500	1000	1500	2000	2500	5000	>5000
Thickness (m)	1350	225	105	75	60	45	22.5 - 30	<22.5
East-West Models								
Width (m)	100	500	1000	1500	2000	2500	5000	>5000
Thickness (m)	1500	300	150	105	83	68	38	37.5

A

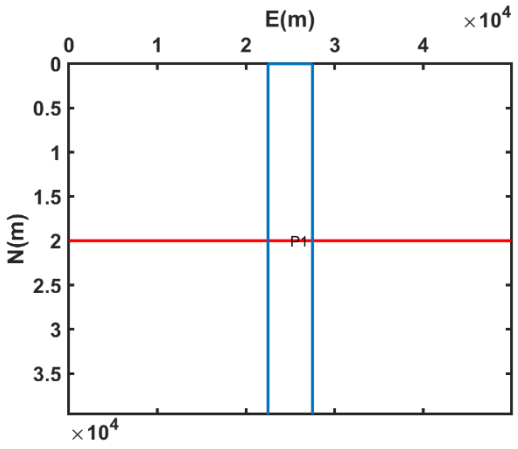

B

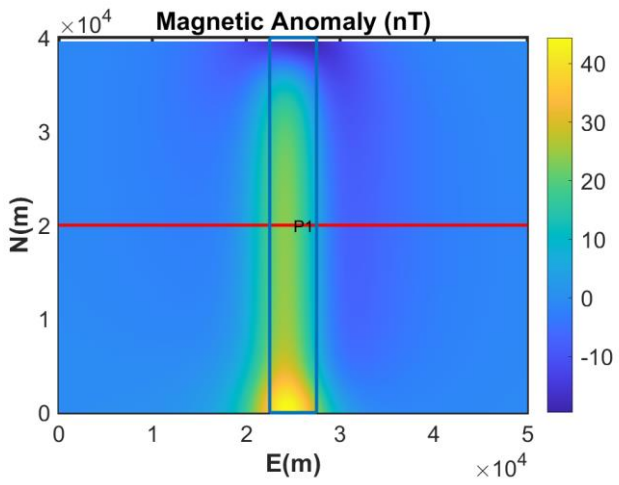

C

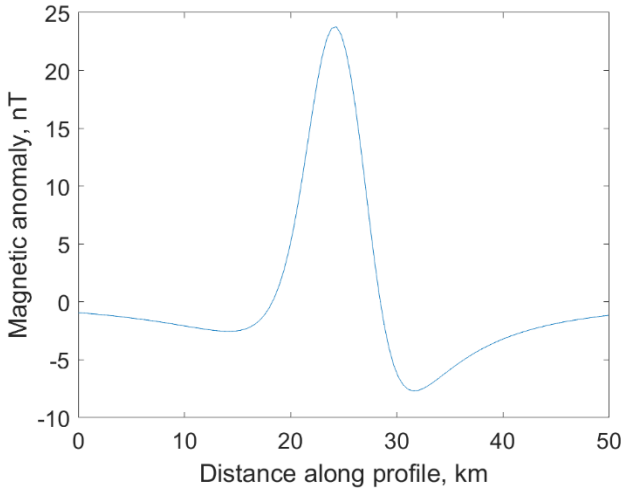

D

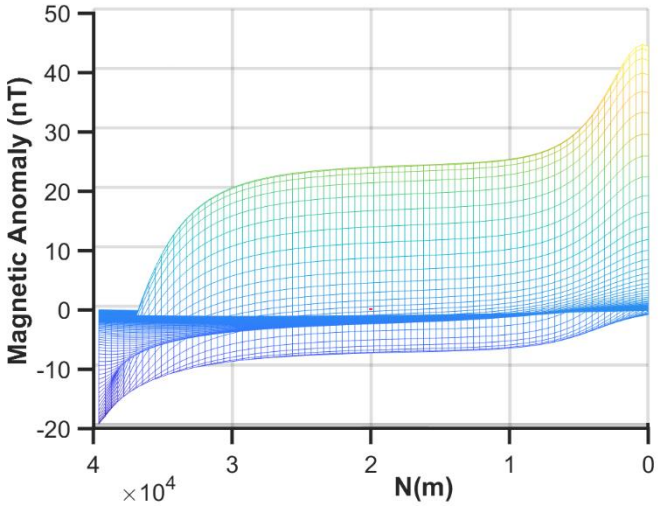

Figure 9. Generic model of an East-West lava flow, 5000 m in width and 38 m thick. A) Box view of the flow dimensions to the east and the north, the red line is the hypothetical track that a ship would take over this flow. B) box view with magnetic anomaly signatures. C) Profile view of the flow, with east-west distance on the x-axis and the magnetic anomaly on the y-axis. D) 2D representation of generic flow looking into the track line, x-axis shows northward distance.

A

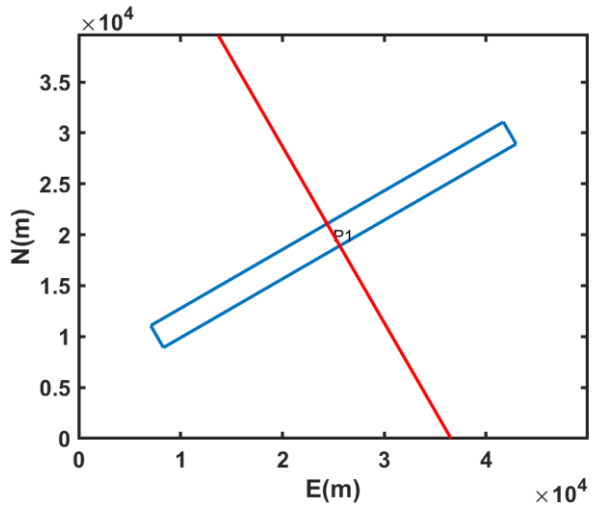

B

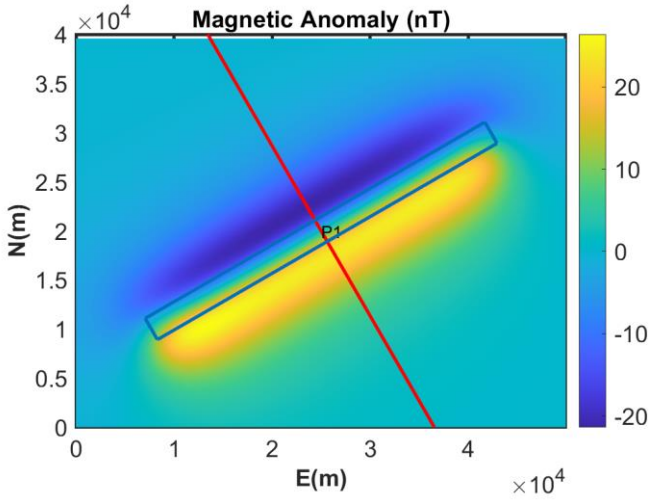

C

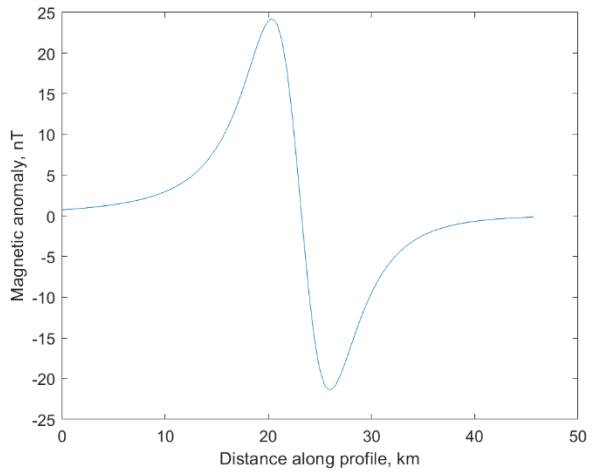

D

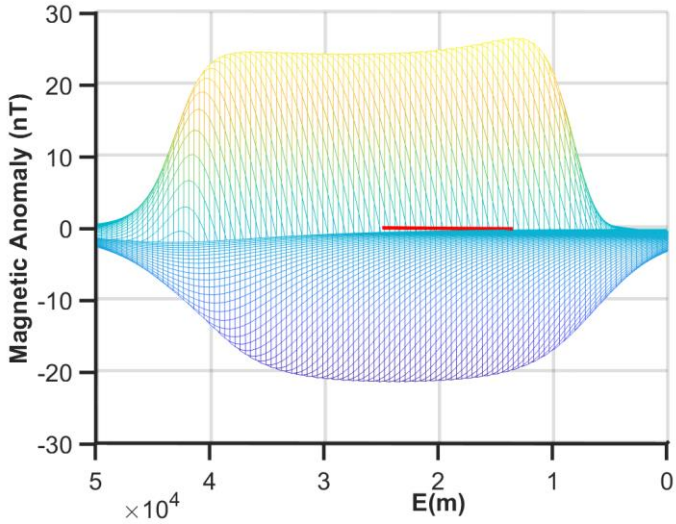

Figure 10. Generic model of a North-South lava flow, all panels have the same description as their East-West counterpart, dimensions of this generic flow were 2500 m in width and 45 m thickness.

The flow that was chosen to model was located on the northern most east-west track line, near the edge of the field (Figures 6 and 8) By manipulating the thickness of each prism, I was able to create a model with reasonable flow thickness (Table 1) that very accurately fit the collected data. This demonstrated that the modeling program was able to use our data to produce a predicted lava flow (Figure 11). The modeled data fits the actual data quite well, except for a small section on the right end of the flow. This discrepancy likely is a result of a nearby lava flow just outside of the survey area and the influence of its own magnetic anomaly (Figure 8).

Table 1. A table showing the thickness value (in meters) assigned to each of the 10 prisms. The results seem to show a fairly thin lava flow that becomes much thinner at the edges.

Prism No.	1	2	3	4	5	6	7	8	9	10
Thickness (m)	5	10	20	30	40	40	50	20	5	5

A

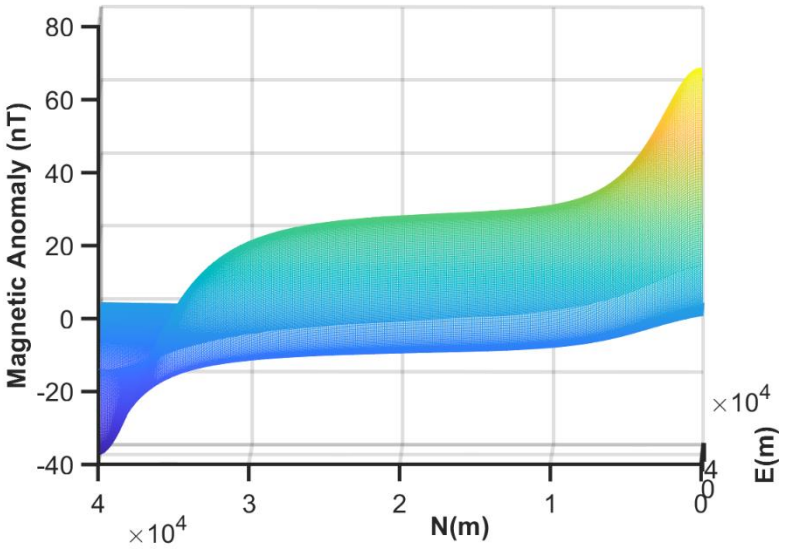

B

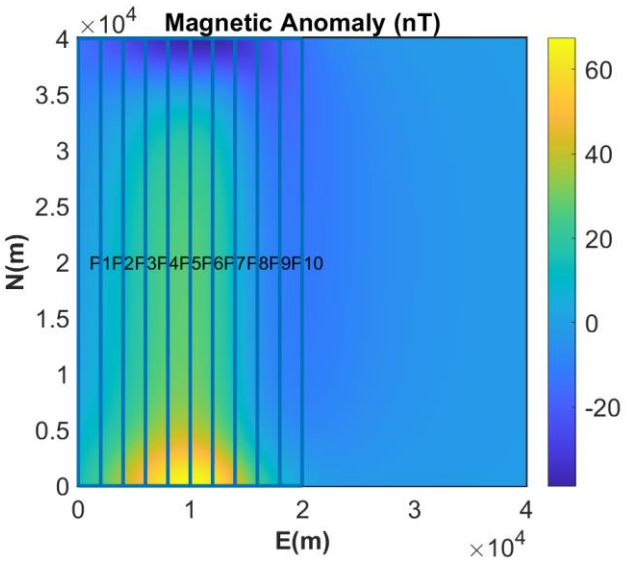

C

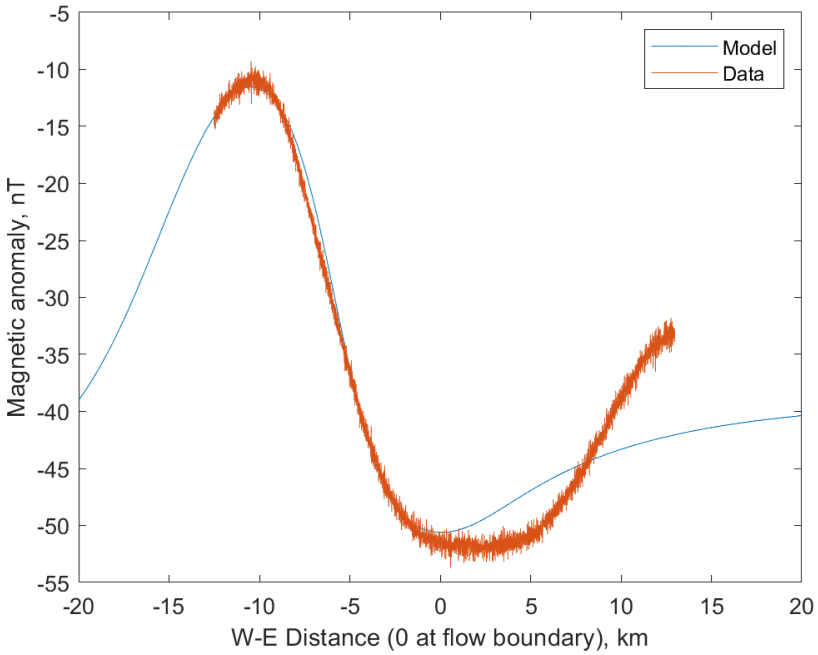

Figure 11. Model of an actual lava flow near the edge of the survey area. A) 2D representation of the flow with distance north on the x-axis, distance east on the z-axis and magnetic anomaly signal on the y-axis. B) Magnetic anomaly over a box view of the flow, showing the 10, 2 km prisms that it was divided into. C) Comparison of the modeled and collected data, there is a very close fit along most of the model, except for near the end. The model cannot be manipulated past this point and there is likely an influence being exerted by another nearby flow that falls just outside of the survey area.

Discussion

The generic models produced first were created to see what size lava flows would be needed to create the anomalies that were detected. A number of these models produced the correct anomaly, but not all were realistic (Table 2). In general, the generic models showed that the real lava flow was not likely to be less than 1-2 km in width, as in order to produce the correct anomaly signal, the flow would have to be unrealistically thick. This was true for both the NS and EW set of generic models, which had a very similar range of acceptable thicknesses. Although, there could be a larger signal from narrower flows if multiple flows were in proximity to one another, as their signals could be combined. There was shown to be a tradeoff between width and thickness (Table 2). While not being exactly 2D models, the generic models roughly fit the elevates changes found in the bathymetry data. Most important to note from these models are the wide range of reasonable dimensions that a flow with an approximate anomaly of ±25 nT could have.

The thicknesses presented in Table 1 show a lava flow that is thicker on the right side, though still relatively thin, which then thins out to around 5 meters at the left edge. A flow of this nature is a reasonable result given what is known about North Arch lava composition and length, which would predict flow thicknesses of 10 meters or more (Gregg and Fornari 1998). This is additionally supported by the presence of a flow front in the northern part of the map that is about 20 meters high. However, as the generic modeling indicated there was a wide range of dimensions that the real lava flow could have had. So, while the model produced (Figure 11) does fit the data quite well, it is likely not the only set of thicknesses that could have done so.

There were a few notable limitations on this study that introduce uncertainty into the results. The remnant magnetization value used was an estimate from a study which measured the

magnetization of Icelandic basaltic magma (Gunnlaugsson et. al. 2006). The remnant magnetization affects the anomaly and therefore the lava flow dimensions, so having a more accurate value would improve the accuracy of my results. This would require collecting lava samples from the North Arch and measuring the magnetization values directly which could not be done in this study due to time and resource limitations. A remnant magnetization of 40 nT was assumed here, other studies on submarine basalts have suggested a value half as large (Fujii and Okino 2018). However, a lower remnant magnetization would have required thicker flows to produce the same anomaly. Since the model indicated that North Arch flows are relatively thin, they appear to be strongly magnetized as well as weaker magnetization would have resulted in thicker flows.

It is also possible that the anomalies detected by the magnetometer were influenced by the underlaying ocean crust, rather than the lava flows themselves. However, this is less likely given the time in which the seafloor around the Hawaiian Islands formed. It is estimated that the lava flows in the North Arch flowed from Cretaceous era ridges (Clague et. al. 1990) were likely created during Cretaceous normal polarity superchron (CNS) (Waggoner 1993). A part of the CNS was the Cretaceous quiet Zone (KQZ), a time in which there was a low frequency of magnetic field polarity reversals and an estimated Vertical Axis Dipole Moment (VADM) of 5.6 $\pm$ 3.2 x 10^{22} Am^2 (Yoshimura 2022), while Earth's current dipole moment is 8 x 10^{22} Am^2. The relative lack of reversals during the KQZ means that this part of the seafloor would contain few magnetic anomalies. If this part of the seafloor had greater variation, it would have been extremely difficult, if not impossible, to detect the anomalies produced by lava flows.

The anomalies of the lava flows could also have been affected by magnetic reversals, which introduces more uncertainty into the model. Flows in the North Arch are predicted to be

between 0.75 – 2.7 Ma, with age decreasing moving away from the Hawaiian Islands (Clague et. al. 1990). The sampled flow is in the southern end of the field and is therefore on the younger end and liked formed in the late Pliocene to early Pleistocene. During the Cenozoic Era, which the Pliocene and Pleistocene were a part of, there were 2-3 magnetic reversals every million years, and the most recent reversal was 770,000 years ago (Ogg 2020). Given that I am only looking at a relatively small section of lava, it is unlikely that there was a magnetic reversal during the emplacement of this section. The flow I analyzed had normal magnetization, but other flows could have had reversed magnetizations.

Another limitation of this project was that it had to be done by creating 2D models in 3D code. While sufficient for a preliminary study, any future work that wishes to go more in depth should use 3D modeling. This will improve the accuracy of the model and give a better image of the modeled flow. The model could also be enhanced by making the resolution of the prisms greater. The prisms in this model were all 10 km in width; a better model would ideally have denser profiles.

Conclusion

The goal of this study was to determine if lava flows in the North Arch Volcanic Field produced strong enough anomalies to produce a model of one of the flows to resolve its thickness. I was able to show that the flows did have strong enough anomalies and that this type of survey can produce a plausible model with data collected from sea surface level, rather than a bottom survey. The final model matched the collected data across one flow boundary with high degrees of accuracy and produced a flow with reasonable thicknesses given the location flow and the viscosity of the lava when it was emplaced. There is still some uncertainty in the data, however. The remnant magnetization of the lava had to be estimated and there is a possibility

that a magnetic field reversal occurred while the flow was cooling. Both factors could have a significant impact on the anomalies produced and therefore the modeled thickness. Any future work would benefit from sampling the flows to directly determine remnant magnetization. As well as by using a 3D model, as opposed to 2D, with denser profiles to give a higher resolution.

Acknowledgements

I would like to thank Professor William Wilcock at the University of Washington for his invaluable help and guidance in this study. I would like to thank the captain and crew of the R/V Thomas G. Thompson, the ship on which this study took place. And I would like to thank Helena Pfluger, Naomi Wu, and Alex Larson for their help in data collection and processing.

References

Ballmer, M. D., G. Ito, J. van Hunen, and P. J. Tackley. 2011. Spatial and temporal variability in Hawaiian hotspot volcanism induced by small-scale convection. Nature Geoscience **4**: 457–460. doi:10.1038/ngeo1187

Bianco, T. A., G. Ito, J. M. Becker, and M. O. Garcia. 2005. Secondary Hawaiian volcanism formed by flexural arch decompression. Geochemistry, Geophysics, Geosystems **6**. doi:10.1029/2005GC000945

Bongiolo, A., J. Souza, F. Ferreira, and L. Castro. 2013. Grav_mag_prism: A MATLAB®/octave program to generate gravity and magnetic anomalies due to rectangular prismatic bodies. Revista Brasileira de Geofisica **31**: 347–363. doi:10.22564/rbgf.v31i3.310

Clague, D. A., K. Uto, K. Satake, and A. S. Davis. 2002. Eruption Style and Flow Emplacement in the Submarine North Arch Volcanic Field, Hawaii, p. 65–84. *In* Hawaiian Volcanoes: Deep Underwater Perspectives. American Geophysical Union (AGU).

Clague, D. A., R. T. Holcomb, J. M. Sinton, R. S. Detrick, and M. E. Torresan. 1990. Pliocene and Pleistocene alkalic flood basalts on the seafloor north of the Hawaiian islands. Earth and Planetary Science Letters **98**: 175–191. doi:10.1016/0012-821X(90)90058-6

Eldholm, O., and M. F. Coffin. 2016. Volcanism and Climate, p. 913–917. *In* J. Harff, M. Meschede, S. Petersen, and Jö. Thiede [eds.], Encyclopedia of Marine Geosciences. Springer Netherlands.

Fujii, M., and K. Okino. 2018. Near-seafloor magnetic mapping of off-axis lava flows near the Kairei and Yokoniwa hydrothermal vent fields in the Central Indian Ridge. Earth, Planets and Space **70**: 188. doi:10.1186/s40623-018-0959-5

Gunnlaugsson, H. P., Ö. Helgason, L. Kristjánsson, P. Nørnberg, H. Rasmussen, S. Steinþórsson, and G. Weyer. 2006. Magnetic properties of olivine basalt: Application to Mars. Physics of the Earth and Planetary Interiors **154**: 276–289. doi:10.1016/j.pepi.2005.09.012

Granot, R., L. Tauxe, J. S. Gee, and H. Ron. 2007. A view into the Cretaceous geomagnetic field from analysis of gabbros and submarine glasses. Earth and Planetary Science Letters **256**: 1–11. doi:10.1016/j.epsl.2006.12.028

Gregg, T. K. P., and D. J. Fornari. 1998. Long submarine lava flows: Observations and results from numerical modeling. Journal of Geophysical Research: Solid Earth **103**: 27517–27531. doi:10.1029/98JB02465

Helo, C. 2016. Explosive Volcanism in the Deep Sea, p. 241–247. *In* J. Harff, M. Meschede, S. Petersen, and Jö. Thiede [eds.], Encyclopedia of Marine Geosciences. Springer Netherlands.

Holcomb, R. T., J. G. Moore, P. W. Lipman, and R. H. Belderson. 1988. Voluminous submarine lava flows from Hawaiian volcanoes. Geology (Boulder) **16**: 400–404. doi:10.1130/0091-7613(1988)016<0400:VSLFFH>2.3.CO

Kearey, P., M. Brooks, and I. A. Hill. 1984. An introduction to geophysical exploration.

Koschinsky, A. 2016. Hydrothermal Vent Fluids (Seafloor), p. 339–344. *In* J. Harff, M. Meschede, S. Petersen, and Jö. Thiede [eds.], Encyclopedia of Marine Geosciences. Springer Netherlands.

McClinton, J. T., S. M. White, A. Colman, K. H. Rubin, and J. M. Sinton. 2014. The role of crystallinity and viscosity in the formation of submarine lava flow morphology. Bulletin of Volcanology **76**: 854. doi:10.1007/s00445-014-0854-2

Normark, W. R., and G. G. Shor. 1968. Seismic reflection study of the shallow structure of the Hawaiian Arch. Journal of Geophysical Research **73**: 6991–6998. doi:10.1029/JB073i022p06991

Ogg, J. 2020. Geomagnetic Polarity Time Scale, p. 159–192. *In*.

Straume, E.O., Gaina, C., Medvedev, S., Hochmuth, K., Gohl, K., Whittaker, J. M., et al. (2019). GlobSed: Updated total sediment thickness in the world's oceans. Geochemistry, Geophysics, Geosystems, 20. DOI: 10.1029/2018GC008115

Pfluger, H. 2022. Bathymetry and Sub-Surface Imaging of the Margins of Effusive Lava Flows in the North Arch.

Tivey, M. A., H. P. Johnson, A. Bradley, and D. Yoerger. 1998. Thickness of a submarine lava flow determined from near-bottom magnetic field mapping by autonomous underwater vehicle. Geophys.Res.Lett. **25**: 805–808. doi:10.1029/98GL00442

Waggoner, D. 1993. The Age and Alteration of Central Pacific Oceanic Crust near Hawaii, Site 843. Proc. Ocean Drill. Program Sci. Results **136**. doi:10.2973/odp.proc.sr.136.212.1993

Wallin, B. H. 1982. The Northern Hawaiian Deep and Arch: Interpretation of Geologic History from Reflection Profiling and Echo Character Mapping. University of Hawaii.

White, W. M. 2016. Hot Spots and Mantle Plumes, p. 316–327. *In* J. Harff, M. Meschede, S. Petersen, and Jö. Thiede [eds.], Encyclopedia of Marine Geosciences. Springer Netherlands.

Yamamoto, M., and J. P. Morgan. 2009. North Arch volcanic fields near Hawaii are evidence favouring the restite-root hypothesis for the origin of hotspot swells. Terra Nova **21**: 452–466. doi:10.1111/j.1365-3121.2009.00902.x

Yoshimura, Y. 2022. The Cretaceous Normal Superchron: A Mini-Review of Its Discovery, Short Reversal Events, Paleointensity, Paleosecular Variations, Paleoenvironment, Volcanism, and Mechanism. Frontiers in Earth Science **10**.